

Response of high rise RC structure with weak beam considering the deterioration due to cyclic behavior under long period earthquake

T.M. MUKAI, T.S. SAITO & H.F. FUKUYAMA

Building Research Institute, Japan

T.Y. YANG

University of British Columbia, Canada



SUMMARY:

High rise building subjected to long period earthquakes may suffer significant damages including non-structural components which are affected by the large inter-story drift. In order to predict the response of high rise buildings during long period earthquakes as accurately as possible, it is necessary to develop the hysteresis model which considers the strength deterioration and energy dissipation deterioration occurred during the cyclic behavior. This paper focuses on the development of a newly proposed hysteresis model for reinforced concrete beams used in high rise building. The hysteresis model is developed based on actual experimental test results. It is shown that this hysteresis model depends on the ratio of ultimate shear strength to ultimate flexural strength and ductility factor and numbers of cycle. The dynamic analysis using the proposed hysteresis model is performed and the influence of difference of hysteresis parameter is discussed.

Keywords: long-period earthquake, RC high rise building, hysteresis model, cyclic deterioration

1. INTRODUCTION

High rise building subjected to long period earthquakes is likely to suffer significant damage to the non-structural components. An actual strong motion was recorded by Building Research Institute in Japan from a 55-story office building located at 770 km away from the hypocenter during the 2011 Tohoku earthquake (BRI 2011). This ground motion doesn't have a high peak ground displacement (less than 10 cm), but the building experienced a large total displacement of 130 cm at the 52nd floor. This large displacement is due to the excessive cyclic behavior caused by the long period earthquake on this high rise building. The long duration (over than 5 minutes) of shaking may have caused many inelastic cyclic to the structural components.

On the other hand, many hysteretic models have been proposed over the years with the purpose of characterizing the mechanical nonlinear behavior of structural components and estimating the seismic response of structural systems. Available hysteretic models range from simple elasto-plastic models to complex strength and stiffness degrading curvilinear hysteretic models (FEMA2009). However, there are few hysteresis models developed in the past for RC member with high strength material, which can consider the cyclic degradation.

It is necessary to develop the hysteresis model of structural components used in the dynamic analysis to consider the strength deterioration and energy dissipation deterioration during the many cyclic loading of the structure. This paper proposes a new hysteresis model for reinforced concrete beam used in high rise building in Japan. The nonlinear hysteresis behaviors are calibrated to match the experimental tests conducted by the Building Research Institute and other institutions (Mukai et al., 2010).

2. OUTLINE OF EXPERIMENTAL TEST AND RESULTS

2.1. Outline of Test Specimen

The experimental test described in this paper was carried out by BRI and other collaborators [Mukai et al., 2010]. Figure 2.1 shows the arrangement of specimens and Table 2.1 shows the detailed parameters for each specimen. Table 2.2 shows the mechanical properties of material used in this specimen. The tested specimen represents a half scale beam at the lower story of a high rise building. The building height is assumed to be 100 meters. There are a total of 8 specimens tested, 5 specimens were tested with 10 cycles of each target displacement, while the remaining 3 specimen were tested with only 2 cycles of each target displacement. The intentional variables in experiments are: 1) number of cycles in loading, 2) amount of longitudinal bar and shear reinforcement, 3) whether or not slab is provided. All specimens are designed to fail in flexure and Table 2.3 shows the ratio (shear safety margin α) of the ultimate shear strength to the shear force when the beam reaches ultimate state in flexural and the shear safety margin α is calculated using Architectural Institute of Japan (AIJ) guideline (AIJ 1999). This is a common design parameter used in practical design for high-rise building in Japan. The plastic rotation angle R_p is given by AIJ guideline which is calculated using the reduction factor for ultimate shear strength. In this study, the R_p is assumed as 0 when the ultimate shear strength is calculated. To calculate the ultimate shear strength for the specimen with slab, AIJ guideline provides a certain value as effective slab width, despite the slab has compressive stress or tensile stress. Some past experimental data showed that when slab has compressive stress, the ultimate shear strength should increase greater than the suggested value. Considering above results in this paper, when slab side has tensile stress, effective width is regarded as width of beam in the calculation of ultimate shear strength.

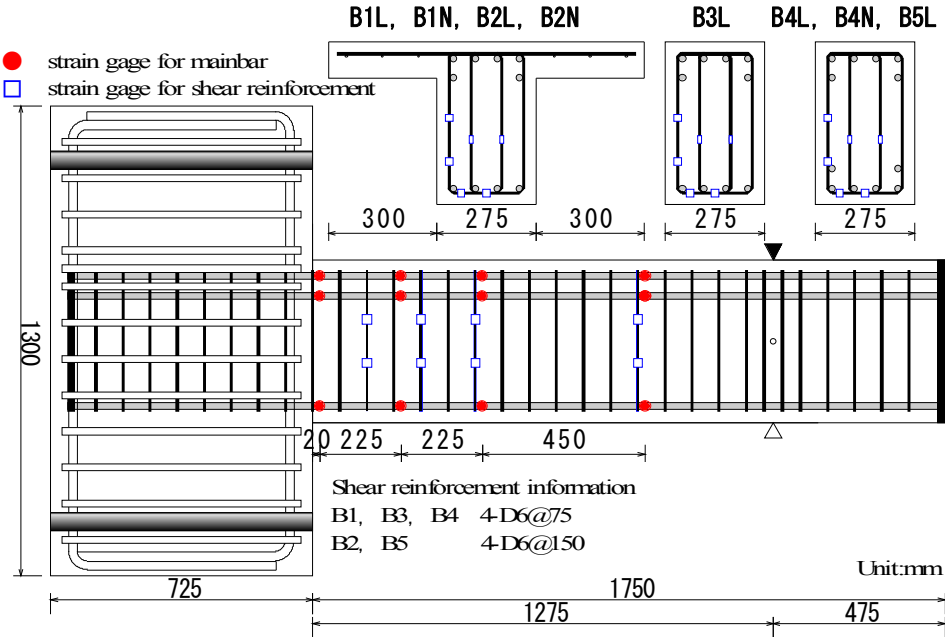


Figure 2.1. Arrangement of reinforcements and strain gauges pasted on reinforcements

Table 2.1. List of Specimens

Specimen	Width	Depth	fc' in design	fc' given by test	thickness of slab	width of slab	reinforcement of slab	Longitudinal bar (tensile reinforcement ratio ρ_t)	Shear reinforcement (shear reinforcement ratio ρ_w)
	mm	mm	N/mm ²	N/mm ²	mm	mm	SD295A	SD490	U 685
B1L	275	450	42	49.4	100	300	3×2-D6	6-D19 (1.39%) 4-D19 (0.93%)	4-D6@75 (0.62%)
B1N				52.4					
B2L				53.8					
B2N				53					
B3L				61.2	-	-	-	6-D19 (1.39%) 6-D19 (1.39%)	4-D6@75 (0.62%)
B4L				54					
B4N				62.6					
B5L				54.2					4-D6@150 (0.31%)

Table 2.2. Mechanical Properties of Material

Reinforcement			
steel bar	yield stress N/mm ²	Young's Modulus kN/mm ²	max tensile stress N/mm ²
D6(SD295A) slab reinforcement	355	198	520
D6(U685) shear reinforcement	763	200	1000
D19(SD490) longitudinal reinforcement	546	191	723

Concrete			
specimen	Compressive stress N/mm ²	Young's Modulus kN/mm ²	tensile stress N/mm ²
B1L	49.4	33.7	3.4
B1N	52.4	38.9	3.6
B2L	53.8	34.2	3.8
B2N	53.0	31.2	4.1
B3L	61.2	34.7	3.6
B4L	54.0	37.1	4.2
B4N	62.6	38.2	3.9
B5L	54.2	36.2	4.0

Table 2.3. Ultimate Strength of Specimens

Specimen			B1L SC* ST*	B1N SC ST	B2L SC ST	B2N SC ST	B3L UC* UT*	B4L	B4N	B5L
Q _{bu}	Ultimate flexural strength for beam	kN	215 279	216 280	216 280	216 280	193 261	267	266	264
V _u	Ultimate shear strength for beam (R _p =0)	kN	830 618	846 631	532 405	532 406	678 678	699	697	507
α_1	Shear safety margin Ultimate shear strength / Ultimate flexural strength		3.86 2.22	3.92 2.25	2.46 1.45	2.46 1.45	3.51 2.60	2.62	2.62	1.92

*SC: in case of slab in compression, *ST: in case of slab in tension

*UC: in case of upper longitudinal reinforcements in compression

*UT: in case of upper longitudinal reinforcements in tension

2.2. Experimental Testing Protocol

The specimen is assumed to have an inflection point at the mid span of the beam. Hence the test setup is prepared such that a concentrated point load is applied at the mid span of the beam. The specimen is subjected to static reversal cyclic displacement load as shown in Figure 2.2. In the general static loading test in Japan, the number of cycles is 2 at each drift angle. For earthquake with long period

components and long duration, a larger number of loading cycles is added. The equivalent cyclic number on a long period earthquake is determined based on the study presented by Mukai et al. (2000). As a result, the number of loading cycle is increased from 2 to 10 for the drift angle at 0.5, 1.0, 2.0, 3.0 %. Figure 2.2 shows the comparison of the loading history. Figure 2.3 shows the location of the instrumentation. The horizontal and vertical displacement at loading point and deformation components are measured. The strain of longitudinal and shear reinforcement are also measured (see Figure 2.1). Horizontal load is measured by load cell.

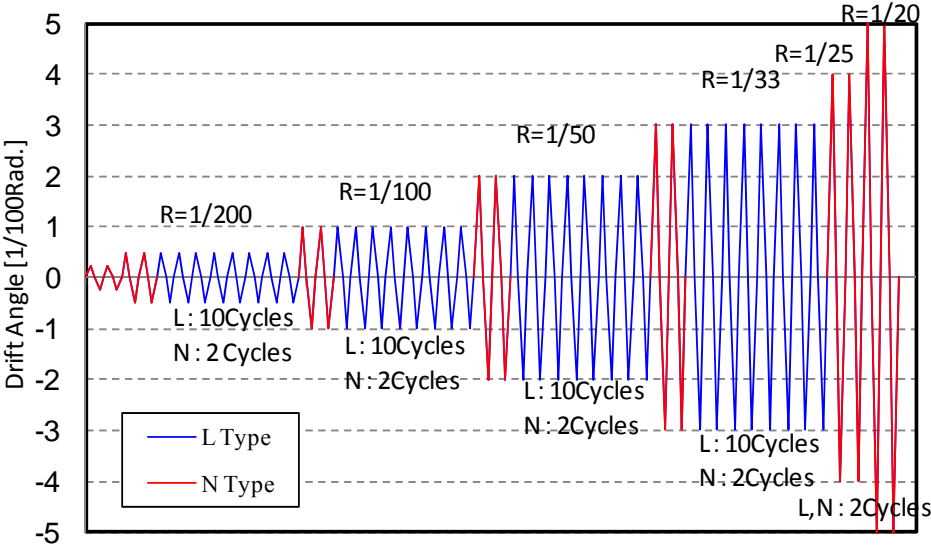


Figure 2.2. Loading history

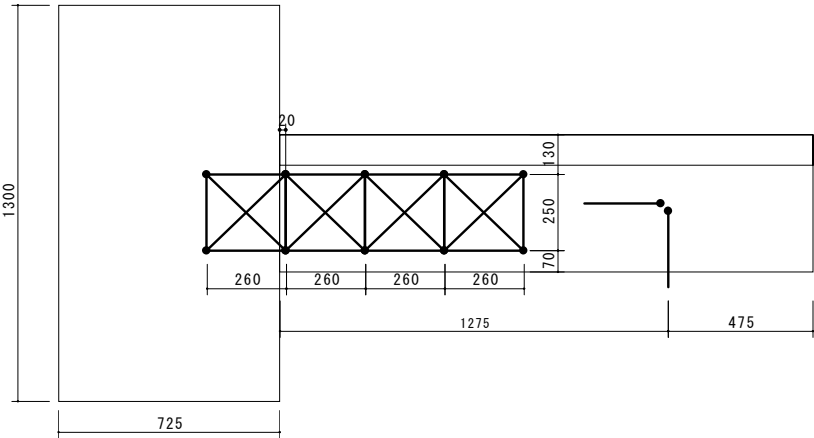


Figure 2.3. Arrangement of displacement transducer

2.3. Test Results

Figure 2.4 shows the force-deformation response of the data measured from each of the specimens. The horizontal axis represents the drift angle and vertical axes shows the shear force for all specimens. For beam specimens with slab (B1L, B1N, B2L, B2N), the lower longitudinal reinforcement at critical section yielded at a drift ratio of approximately 1% and reached maximum strength at 2%, the deterioration of strength on each backbone curve didn't occur in compression side of slab (the first quadrant in the figure). On the other hand, the upper longitudinal reinforcements yielded at -1% and the strength deterioration on each backbone curve didn't occur excluding B2L specimen in tension side of slab (the third quadrant). The shear reinforcement yielded at a drift ratio of -4% for B1L, at -5% for B1N, at -2% for B2L, at -3% for B2N respectively.

For rectangular beam specimens (B3L, B4L, B4N, B5L), the longitudinal bar at critical section yielded same as the specimen with slab and the strength deterioration on each backbone curve didn't occur excluding B5L specimen. The shear reinforcement yielded at -3% for B5L.

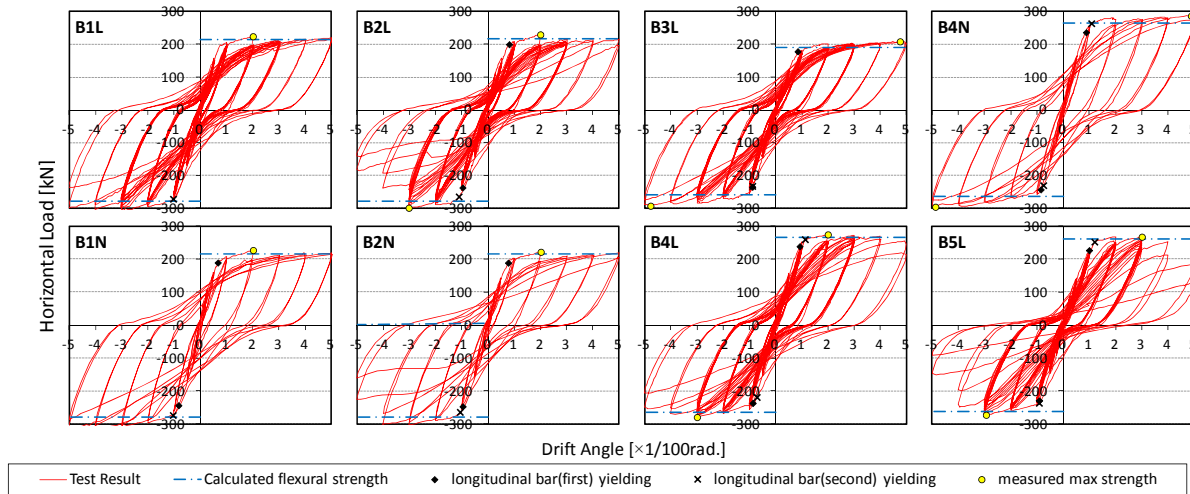


Figure 2.4. Shear – drift ratio response for all beam specimens

3. PROPOSAL ON HYSTERESIS MODEL CONSIDERING CYCLIC DETERIORATION

3.1. Classification of Deterioration Behavior

According to the test results described in section 2, there are some classifications of deterioration as shown in Fig 3.1. 1): deterioration of backbone curve; 2): deterioration of the strength due to cyclic behavior (In-cycle strength deterioration); 3): deterioration of hysteresis due to energy dissipation in the second cycle; 4): hysteresis energy dissipation deterioration ratio due to cyclic behavior (In-cycle energy dissipation deterioration). Note that the hysteresis energy dissipation deterioration ratio by the deterioration of strength ratio due to cyclic behavior should be ignored to avoid evaluating the deterioration of hysteresis energy dissipation twice.

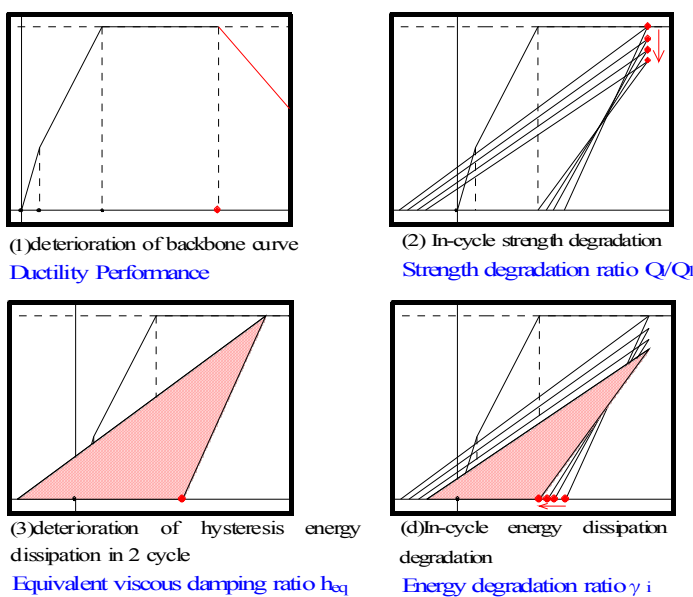


Figure 3.1. Category of deterioration for RC member

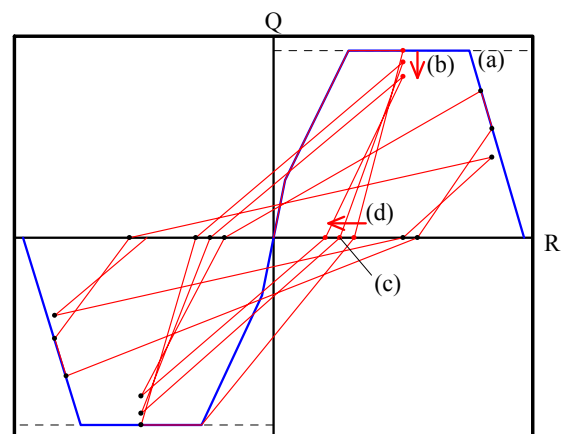


Figure 3.2. Proposed hysteresis rule

3.1.1. Deterioration of backbone curve

The test results of B2L imply that there is relationship between the shear margin ratio and deterioration of backbone curve due to cyclic behavior. The cause of deterioration should be assumed by the degradation of hinge zone due to cyclic behavior. As mentioned in section 2.1, the ultimate shear strength calculated based on AIJ guideline is given by using a plastic rotation angle R_p . Here, a new deterioration coefficient β is introduced and to be multiplied to R_p to simulate the deterioration of the backbone curve due to cyclic response.

$$\beta = \frac{N}{8}(0.32\alpha - 0.76) - \frac{1}{4}(0.32\alpha - 4.76) \quad (\beta \leq 1.0) \quad (3-1-1)$$

N is the cyclic number [times]; α is the shear safety margin; β is the deterioration coefficient for backbone.

3.1.2. In-cycle strength deterioration

The test results showed that in-cycle strength deterioration depends on only the cyclic number N at before-yielding displacement range ($1/200 < R < 1/100$), the cyclic number N and the ductility factor, the shear safety margin α at more displacement range ($1/100 < R$). Additionally, the in-cycle strength deteriorates severely up to $N=5$, after that, the degree of deterioration show a gradual decline. The following equations shows the in-cycle strength deterioration ratio, Before yielding displacement range ($1/200 < R < 1/100$):

$$Q_i / Q_1 = 0.0040(N - 5)^2 + 0.936 \quad N=1 \sim 5 \quad (3-1-2)$$

$$Q_i / Q_1 = -0.0042(N - 5) + Q_5 / Q_1 \quad N=6 \sim 10 \quad (3-1-3)$$

After yielding displacement range corresponding to ductility factor 1 to 2 ($1/100 < R < 1/50$):

$$Q_2 / Q_1 = a_2 Q_1 \quad N=2 \quad (3-1-4)$$

$$Q_i / Q_1 = -0.0080(\mu / \alpha)^{1.7}(N - 2) + Q_2 / Q_1 \quad N=3 \sim 5 \quad (3-1-5)$$

$$Q_i / Q_1 = -0.0070(\mu / \alpha)^{2.3}(N - 5) + Q_5 / Q_1 \quad N=6 \sim 10 \quad (3-1-6)$$

$$a_2: 0.85 \text{ (In case that slab has compression stress), } 0.95 \text{ (other cases)}$$

After yielding displacement range corresponding to ductility factor 2 to 3 ($1/50 < R < 1/33$):

$$Q_i / Q_1 = -0.0080(\mu / \alpha)^{1.7}(N - 1) + 1 \quad N=2 \sim 5 \quad (3-1-7)$$

$$Q_i / Q_1 = -0.0070(\mu / \alpha)^{2.3}(N - 5) + Q_5 / Q_1 \quad N=6 \sim 10 \quad (3-1-8)$$

N is the cyclic number [times]; α is the shear safety margin; μ is the ductility factor.

3.1.3. Deterioration of hysteresis energy dissipation in the second cycle

The hysteresis energy dissipation performance could be expressed by equivalent hysteresis damping factor h_{eq} generally. The test results shows that h_{eq} is constant value of approximately 5 % within elastic state, increases significantly up to $R=1/50$ (when $\mu=2$) and increases moderately after that point. Additionally, h_{eq} is related to shear safety margin α and, as α increases, h_{eq} increases. The equation for hysteresis energy dissipation deterioration is proposed as followings,

$$h_{eq} (\%) = 5 \quad \mu < 1 \quad (3-1-9)$$

$$h_{eq} (\%) = (3.4\alpha + 2.3)\mu - 3.4\alpha_1 + 2.7 \quad 1 \leq \mu < 2 \quad (3-1-10)$$

$$h_{eq} (\%) = 3.4\alpha + 7.3 \quad \mu \geq 2 \quad (3-1-11)$$

3.1.4. In-cycle energy dissipation deterioration

In this paper, in-cycle energy dissipation deterioration expressed as the ratio of the energy dissipation E_i in i th cycle to the energy dissipation in the second cycle E_2 . This ratio includes the deterioration of hysteresis energy due to not only in-cycle strength deterioration but also the deterioration of unloading stiffness. The former has already considered by the equation proposed in 3.1.2 and must be eliminated to express only in-cycle energy dissipation deterioration. In this regards, the in-cycle energy dissipation deterioration should be defined using energy dissipation deterioration ratio $\gamma_i = (E_i/Q_i)/(E_2/Q_2)$, where Q_i and Q_2 are the peak strength of at the i th cycle and second cycle, respectively.

The test result shows that γ_i decreases up to approximately 4th cycle, after that this value remains constant value in the small displacement range. Such number does not decrease even after 10 cycles of large displacement.

Based on these observations, the following equations are proposed as energy dissipation deterioration ratio.

$$\frac{(E_i/Q_i)}{(E_2/Q_2)} = (-0.005\mu \cdot \alpha + 0.075)(N-4)^2 + 0.020\mu \cdot \alpha + 0.7 \quad N=2 \sim 4 \quad (3-1-12)$$

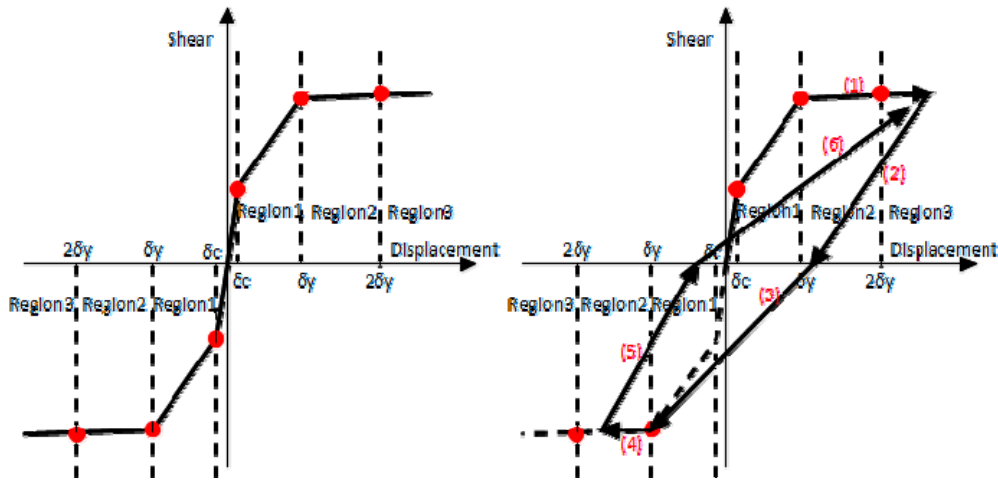
$$\frac{(E_i/Q_i)}{(E_2/Q_2)} = (-0.0078\mu/\alpha - 0.015)(N-4) + \frac{(E_4/Q_4)}{(E_2/Q_2)} \quad N=5 \sim 10 \quad (3-1-13)$$

4. DYNAMIC ANALYSIS AND RESULTS

The nonlinear dynamic analysis of a SDOF using the proposed hysteresis model is performed to compare the response behavior between a proposed model and existing models. The Modified Takeda model (Takeda et al 1970) and Simplified Takeda model were used in this analysis as existing model. The Simplified Takeda model is used in this paper where the difference between Modified Takeda model and Simplified Takeda model is the hysteresis rule before displacement reaches the yielding point and the points for Simplified model before yielding point heads to origin under unloading. The ground motion (MLIT 2010) used in this paper includes the long period component with the duration time is 640 sec. The yielding strength of structure is adjusted such that the response of structure reaches a certain plastic deformation level under input motions.

The program for dynamic analysis for SDOF is developed, Newmark β method with recurrence formula and Newton iteration method is used as a numerical integration method. The damping type is proportional to initial stiffness and damping factor is 5%. Each cyclic number corresponding to displacement level can be counted in this program when structure reaches in each region at positive and negative side (see Figure 4.1(a)). If structure behaves under earthquake like figure 4.1(b), each cyclic number pN_i , nN_i at positive and negative changes like Table 4.1. Thus, it is assumed that the cyclic deterioration happens when structure reaches in same both displacement regions in this study.

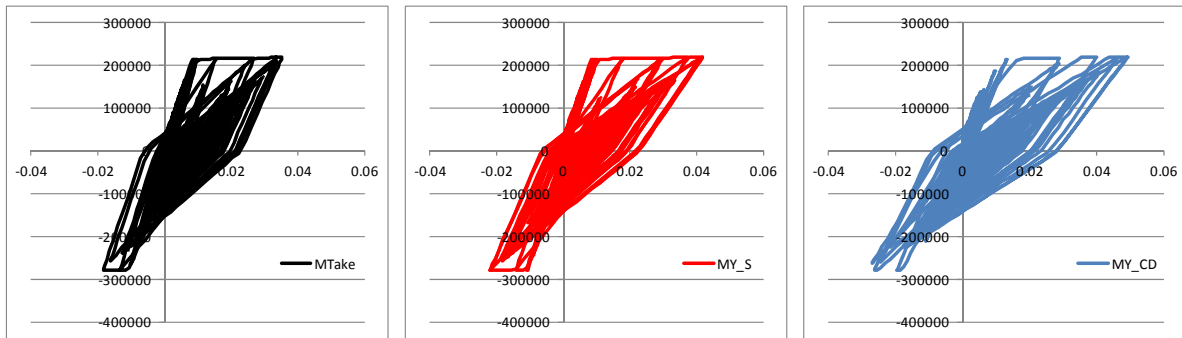
Figure 4.2 shows a result of dynamic analysis with each hysteresis model. The maximum response displacement of Cyclic Deterioration model is 1.37 times as large as Modified Takeda model due to cyclic deterioration behavior under same input motion. Thus, it is confirmed that this proposed hysteresis model can express the cyclic deterioration behavior under long period earthquake and makes it clear the difference of response obtained by an existing hysteresis model. The investigation on accuracy of the proposed hysteresis model by other test data will be an issue in the future.



(a) Each region for count of the cyclic number (b) Example on count of each cyclic number
Figure 4.1. Count rule of cyclic number

Table 4.1. Change of Each Cyclic Number

Segment	Cyclic Number					
	Positive side			Negative side		
	pN1	pN2	pN3	nN1	nN2	nN3
(1)	1	1	1	0	0	0
(2)	1	1	1	0	0	0
(3)	1	1	1	1	0	0
(4)	1	1	1	1	1	0
(5)	1	1	1	1	1	0
(6)	2	2	1	1	1	0



(a) Modified Takeda Model (b) Simplified Model (c) Cyclic Deterioration Model
Figure 4.2. Dynamic analysis result under long period earthquake ($C_0=0.05$, $\alpha=2.0$ $T=0.82$)

5. CONCLUSIONS

This paper proposed a new hysteresis model to simulate the cyclic deterioration behavior of the reinforced concrete beams used in the high rise construction in Japan. The failure mode of specimens tested was flexural failure. The force-deformation response deterioration was classified into 4 types. Empirical formulas were developed to simulate these responses. A new hysteresis model incorporating these new parameters was developed. The result of dynamic analysis showed the proposed analytical model is possible to calculate the response considering the many inelastic cyclic behavior which will make a significant impact to the assessment of high-rise RC building under long-period earthquakes.

ACKNOWLEDGEMENT

The work was carried out in part by the Building Research Institute, Kumagaigumi Co., Ltd, Hazama Corporation, Toda Corporation, Nishimatsu Construction Co., Ltd, Fujita Corporation, Sato Kogyo Co., Ltd. using the funding by Ministry of Land, Infrastructure, Transport and Tourism. All sources of funding and support of all institutions and persons concerned are gratefully acknowledged.

REFERENCES

- Architectural Institute of Japan (1999). Design Guidelines for Earthquake Resistant Reinforced Concrete Buildings Based on Inelastic Displacement Concept, Tokyo, Japan. (in Japanese)
- Building Research Institute (2011). Summary of the Field Survey and Research on "The 2011 off the Pacific coast of Tohoku Earthquake" (the Great East Japan Earthquake), BRI Research Paper, No. 150, September
- FEMA P440A (2009). Effects of Strength and Stiffness Degradation on Seismic Response, June
- Ministry of Land, Infrastructure, Transport and Tourism (2010). Public comments on measurements on super high-rise buildings under long period earthquake, December, (in Japanese)
http://www.mlit.go.jp/report/press/house05_hh_000218.html
- Takeda, T., Sozen, M.A. and Nielsen, N.N. (1970). Reinforced Concrete Response to Simulated Earthquakes, Journal of the Structural Division, ASCE, Vol. 96, ST12, pp.2557-2571, December
- Mukai, T., Takahashi, T., Hamada, M., Saito, T., Fukuyama, H., Yagenji, A. and Kinugasa, H., (2010). Study on Strength Degradation for R/C Beams Subjected to High Cyclic Deformations, Journal of Structural Engineering, AIJ, Vol.56B, pp.21-31, March (in Japanese)
- Mukai, T., Kinugasa, H., Nomura, S. (2000). Estimation method of requisite strength to control deformation of RC structure under earthquake motion and investigation accuracy, J. Struct, Constr. Eng., AIJ, No532, pp.137-143, June (in Japanese)